Nanosized tin and tin oxides loaded expanded mesocarbon microbeads as negative electrode material for lithium-ion batteries

Shubin Yang, Huaihe Song [*], Xiaohong Chen

State Key Laboratory of Chemical Resource Engineering, Beijing University of Chemical Technology, 100029 Beijing, PR China

Abstract

Tin-based composites using expanded mesocarbon microbeads (EMCMB) as matrix were prepared by impregnating tin chloride and the following reduction under hydrogen atmosphere at different temperatures. The morphologies and structural characteristics of the composites were investigated by FE-SEM, EDS and XRD measurements. It was found that tin exists inside EMCMB in the form of oxidation states (Sn(II) and Sn(IV)) after reduction at lower temperature (below 350 °C), and metallic tin exists both outside EMCMB and between carbon layers after reduction at higher temperature (450 °C). The electrochemical properties of the composites as negative electrode material for lithium-ion batteries were systematically investigated by cyclic voltammetry, galvanostatic cycling and electrochemical impedance spectroscopy tests. The results showed that loading amount of tin or tin oxides and reduction temperature had large influences on the reversible capacity and cycle performance of these composites. Among them, the composite reduced at 230 °C with appropriate loading amount of tin oxides not only exhibited the high first reversible gravimetric capacity of 401 mAh g^{-1} and an excellent cyclability with only 0.2% capacity loss/cycle at lower current density, but also showed a stable cycle performance at higher current density due to its lower resistance.
© 2007 Elsevier B.V. All rights reserved.

Keywords: Lithium-ion batteries; Mesocarbon microbeads; Tin-based composites; Cycle performance

1. Introduction

Recently, metallic tin and tin oxides as negative electrode materials for lithium-ion batteries have attracted much attention due to their high-theoretical capacities (e.g., Sn: 994 mAh g^{-1} [1], SnO: 876 mAh g^{-1} [2], SnO$_2$: 781 mAh g^{-1} [3]). However, a large specific volume change usually occurs in the host matrix during the charge and discharge process [4], which leads to rapid pulverization of the electrode [5,6] and decrease of electrical conductivity between active material particles. As a result, these materials have not been applied in practical lithium-ion batteries until now. At present, one solution for the problem of easy pulverization and bad cyclability of tin and tin compounds is to search for a suitable matrix which is able to accommodate their volume change [5–15]. Since carbonaceous materials have smaller expansion during charge and discharge process and fair ductility [5,6], they are widely chosen as the matrices of tin-based negative electrode materials to improve their cycle performances.

Tin-mesocarbon microbeads (MCMB) [7], tin–graphite [6] and tin oxides–graphite [5,6] composites using MCMB or natural graphite as the matrices have been prepared and their electrochemical performances have been investigated by many research groups. Their results showed that the use of graphite matrix could improve the cyclability of Sn-based negative electrodes due to the ductility, conductivity and most significantly, the obstruction property of the graphite matrix, which could effectively buffer the volume change during the alloying and dealloying reaction with Li ion. However, a new problem was produced: in these composites tin and tin oxides were usually located on the surface of graphite, and unavoidably aggregated into large particles after long cycle.

Recently, a new trend is to synthesize the tin or tin oxides–carbon composites, in which the tin or tin oxide nanopar-

ticles are confined in the nanopores of mesoporous carbons [8,9], for the purpose of alleviating the agglomeration of nanoparticles and enhancing their cycle performances. For example, Grigoriants et al. [8] have prepared Sn-mesoporous carbon composite using mesoporous carbon as the matrix, and found that the electrode comprising this composite delivers a reversible capacity of 400 mAh g^{-1} at about 0.05 mA cm^{-2}, which is much higher than that of graphite electrodes. But the electric conductivity of these mesoporous carbons is low, and additional binders and conducting agents for providing the electronic connectivity between particles were usually required.

It is well known that graphitized mesocarbon microbeads is an attractive negative electrode material for commercial lithium-ion batteries because of its high capacity at low potential and good cyclability at low charge/discharge rate [16]. By expansion treatment, the high-rate performance of MCMB electrode was improved [17]. In this work, expanded mesocarbon microbeads (EMCMB) with fair electric conductivity and high porosity was prepared from graphitized MCMB for the purpose of using as the matrix of tin or tin oxides. On the basis of comparing the changes of morphology and structure of tin or tin oxides–EMCMB composites after reduction at different temperatures, the electrochemical properties of these composites as negative electrode material for lithium-ion batteries were systematically investigated by cyclic voltammetry (CV), galvanostatic cycling and electrochemical impedance spectroscopy (EIS) tests.

2. Experimental

Graphitized MCMB (manufactured by Osaka Gas Corp., Japan) with an average diameter of 10 μm were added into a 2:1 (weight ratio) mixture of concentrated sulfuric acid and nitric acid. The mixture was stirred at 45 °C for 30 min, and then KMnO$_4$ and FeCl$_3$ (all analytical pure grade) were gradually added to participate in the intercalation reaction with MCMB. After reaction for 12 h, the mixture was filtered, washed and dried. Then the intercalated MCMB were quickly sent to a tubular furnace pre-heated to 900 °C, expansion took place along *c*-axis of MCMB and worm-like EMCMB were generated. 0.8 g of this material was impregnated into a SnCl$_2$/ethanol solution with the different concentrations of 0.5, 1.3 and 1.9 mol L^{-1}, respectively, for 48 h at 25 °C, and the centrifugation residue was washed three times with ethanol in order to eliminate the tin compounds adsorbed on the surface of EMCMB. After the samples were dried at 32 °C, they were heated to certain temperatures (230, 350 and 450 °C) under N$_2$ atmosphere, and then reduced with transferred H$_2$ atmosphere at the same temperatures for certain hours (230 °C for 5 h, 350 °C for 1 h, 450 °C for 30 and 60 min, respectively) in order to convert the impregnated tin compounds into metallic tin particles. Thus the tin-based EMCMB composites (tin oxides–EMCMB or tin–EMCMB) were obtained and denoted as TE-*X-Y*. Here, TE means tin–EMCMB composite, *X* represents the reduction temperature, and *Y* represents the concentration of SnCl$_2$/ethanol solution during the impregnating process.

The morphology and microstructure of the samples were observed by scanning electron microscopy (SEM, Cam-

bridge S-250MK3) and field-emission scanning electron microscopy (FE-SEM, Hitachi S-4700) equipped with energy dispersive X-ray spectroscope (EDS). The X-ray diffraction (XRD) measurements were conducted on a Rigaku D/max-2500B2+/PCX system with Cu Kα radiation ($\kappa = 1.5406$ Å). Brunauer–Emmett–Teller (BET) specific surface areas were determined from N$_2$ adsorption by using a Micromeritics ASAP 2020 (USA) analyzer at liquid nitrogen temperature. The content of tin in the composites was calculated from the weight variation of EMCMB before and after impregnating by changing tin dichloride to metallic tin. A three-electrode system was used in the electrochemical study. Lithium sheets were used as both reference and counter electrodes, and composite electrode prepared by mixing the sample powder with acetylene black as an electrical conductor and polyvinylidene difluoride (PVDF) as a binder in a mass ratio of 90:1:9 was used as working electrode. The round wafer-shaped composite electrodes possess the constant surface area of 1.5 cm^2 and the thickness of 90–100 μm (active material film). 1 mol L^{-1} LiPF$_6$ solution in a 1:1 (volume) mixture of ethylene carbonate (EC) and dimethyl carbonate (DMC) from Merck Co. was used as electrolyte. The cells were galvanostatically charged and discharged over the potential range from 0.01 to 2.50 V versus Li/Li$^+$ at the current densities of 0.2 and 0.8 mA cm^{-2}, respectively. Cyclic voltammetry (CV) and electrochemical impedance spectroscopy (EIS) measurements of the composite electrodes were carried out on an electrochemical workstation (CHI 660B). The cyclic voltammograms were obtained over the potential range from 2.50 to 0.01 V at a scanning rate of 0.1 mV s^{-1}. AC impedance spectra were obtained by applying a sine wave with amplitude of 5.0 mV over the frequency range from 100 kHz to 0.01 Hz. Fitting of the impedance spectra to the proposed equivalent circuit was performed by using the code Zview.

3. Results and discussion

The schematic diagram of the overall synthetic procedure of tin or tin oxides–EMCMB composites is described in Scheme 1.
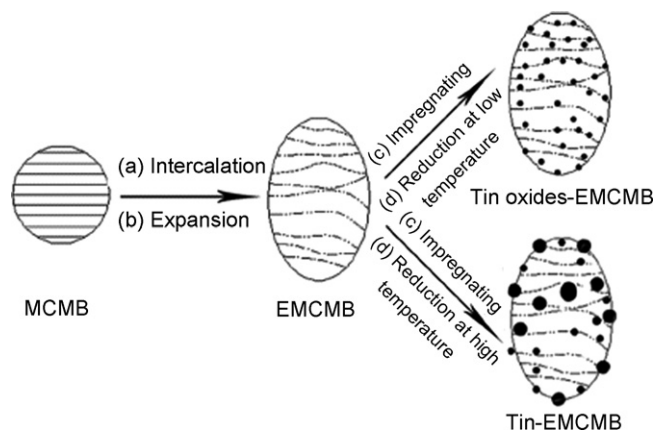
Scheme 1. Schematic diagram of the preparation of tin and tin oxides–EMCMB composites: (a) the formation of intercalated MCMB; (b) expansion treatment at 900 °C; (c) impregnating in SnCl$_2$/ethanol solution; (d) reduction under H$_2$ atmosphere at different temperatures.

According to our previous papers [17,18], through intercalation and expansion treatments graphitized MCMB can be transformed into elliptical EMCMB from original regular spherule. Fig. 1(a) shows that EMCMB exhibits elliptical shape, in which most of the carbon sheets are basically parallel to each other which deform in an irregular pattern. The BET surface area of EMCMB was improved from $1.5\,m^2\,g^{-1}$ for the pristine MCMB to $18\,m^2\,g^{-1}$ and more pores were generated. This material with above characters should be a suitable matrix for Sn-based negative electrodes.
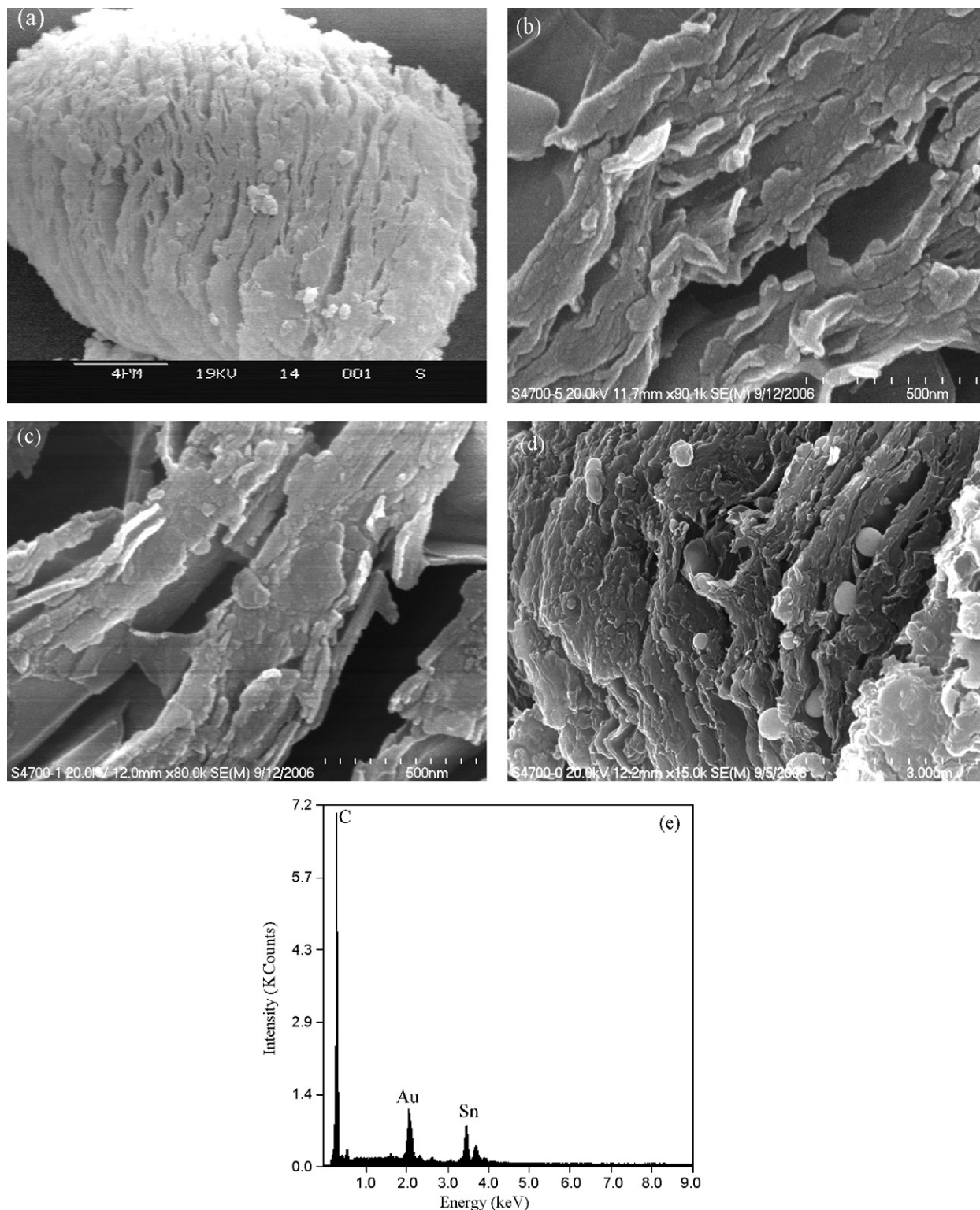

Fig. 1. SEM image of EMCMB (a), FE-SEM images of TE-230-1.3 (b), TE-350-1.3 (c) and TE-450-1.3 reduced for 60 min (d), and typical EDS analysis of TE-450-1.3 reduced for 60 min (e), respectively.
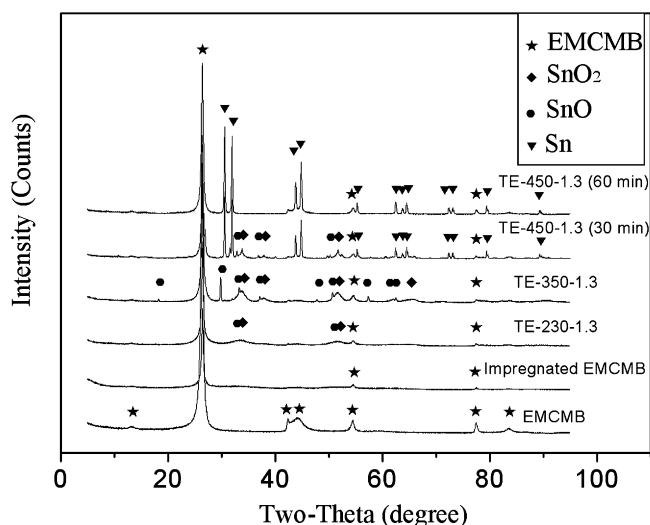
Fig. 2. XRD patterns of EMCMB, SnCl₂ solution impregnated and dried EMCMB, TE-230-1.3, TE-350-1.3 and TE-450-1.3 reduced for 30 and 60 min.

In a typical synthesis of tin or tin oxides–EMCMB composites, SnCl₂·2H₂O was selected as the starting tin source and ethanol as solvent in order to make more tin ion diffuse into the pores of EMCMB. The existing state of tin in composites was controlled by reduction temperature (230, 350 and 450 °C) and the loading amount of tin was altered by changing the concentration of the SnCl₂ solution. The resultant composites containing 7.1, 9.5 and 21.6 wt.% tin were prepared from the SnCl₂ solutions of 0.5, 1.3 and 2.9 mol L⁻¹, respectively.

The XRD patterns of the tin or tin oxides–EMCMB composites are presented in Fig. 2. Compared with the spectrum of EMCMB, for TE-230-1.3 sample, two additional broad and weak diffraction peaks appeared at the ranges of 30–35° and 48–53°, but the peaks corresponding to SnCl₂ at 19.2° and 39.2° are invisible, which means Sn exists in the form of amorphous oxides rather than SnCl₂. With the increase of reduction temperature to 350 °C, the peaks of tin oxides become more intense and can be clearly distinguished in the spectrum of TE-350-1.3, suggesting that the crystalline structure of tin oxides tended towards integrity and their sizes grew up with the increase of temperature. According to JCPDS card, the peaks at $2\theta = 18.3°, 29.8°, 33.3°, 37.1°, 44.4°, 50.7°, 57.4°$ and $62.5°$ are corresponding to the (0 0 1), (1 0 1), (1 1 0), (0 0 2), (1 0 2), (1 1 2), (2 1 1) and (1 0 3) diffraction peaks of SnO, respectively; the peaks at $2\theta = 33.8°, 38.0°, 51.5°, 54.8°, 57.8°$ and $65.9°$ are corresponding to the (1 0 1), (2 0 0), (2 1 1), (2 2 0), (0 0 2) and (3 0 1) diffraction peaks of SnO₂, respectively, indicating that tin species are in the form of oxidation states (Sn(II) and Sn(IV)) at temperature below 350 °C in our samples. The reason for this should be that SnO is nanosized, which is easy to be partially oxidized to Sn(IV) in air [8,19]. The average grain sizes of SnO₂ and SnO in TE-350-1.3, calculated using the Scherrer equation [20] are 10 and 12 nm, respectively. After reduction at 450 °C for 30 min, the peaks of metallic Sn appear except for those of SnO and SnO₂, but the peaks of SnO become very weak. The reason for this should be that SnO is thermodynamically unstable at 450 °C and undergoes the disproportion

reaction shown in the following equation [19]:

$$2SnO(s) = SnO_2(s) + Sn(l) \qquad (1)$$
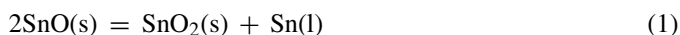
when the reduction time prolongs to 60 min at 450 °C, the peaks of SnO₂ disappear and only the sharp peaks of well-crystallized tin are present, indicating that Sn exists in the form of metallic Sn with the average diameter of 41 nm from calculation after reduction at 450 °C for 60 min.

Fig. 1(b)–(d) shows the FE-SEM images of TE-230-1.3, TE-350-1.3 and TE-450-1.3 reduced for 60 min. From Fig. 1(b) and (c), it can be clearly seen that there are many structural defects on the surface of EMCMB and various cracks between carbon layers, but tin oxides are invisible, indicating that tin oxides are not on the surface of these composites. In contrast, in the FE-SEM image of TE-450-1.3 reduced for 60 min (Fig. 1(d)), there are spherical or elliptical particles with the size of 200–500 nm presenting between carbon layers and on the surface of EMCMB. These particles are the metallic tin, which is confirmed by their spot energy dispersive spectroscopy analysis (Fig. 1(e)), well consistent with its XRD result. The reason for this phenomenon should be that, for the tin-based composites, at lower reduction temperature (below 350 °C), the tin oxides have small average grain sizes (below 12 nm) and are mainly inside EMCMB, on the contrary when the reduction temperature is increased (450 °C), tin oxides are reduced and transformed into liquid metallic Sn, which tends to flow outside and form larger spherical or elliptical particles.

Such different morphology and structure among above composites should lead to the different electrochemical properties when they are used as the negative electrode materials for lithium-ion batteries. To investigate the electrochemical properties, cyclic voltammetry measurements were initially conducted at a scanning rate of 0.1 mV s⁻¹ over the potential range from 2.50 to 0.01 V. The cyclic voltammograms (CVs) are shown in Fig. 3. From Fig. 3(a), it can be seen that, during the first scanning cycle, there are two reduction peaks and one oxidation peak. The first reduction peak in the potential range 0.5–1.0 V is ascribed to the formation of SEI (solid electrolyte interface) film [21] on the surface of EMCMB electrode, which disappears in subsequent cycles; the second reduction peak close to 0.0 V versus Li/Li⁺ is attributed to the insertion of Li⁺ into the layers of EMCMB. And the oxidation peak centered at 0.2 V corresponds to the reversible extraction of Li⁺ from the EMCMB layers. From Fig. 4(b)–(e), it is observed that the CVs of these composites have substantial difference from that of EMCMB, e.g., many additional peaks are present. For TE-350-1.3 and TE-450-1.3 reduced for 30 min, there is an additional reduction wave at 0.9 V prior to the formation of SEI film, which corresponds to the irreversible conversion of SnO₂ to Sn and Li₂O [22]. Interestingly in the CV of TE-230-1.3 this wave at 0.9 V is not distinct and is replaced by a wave at 1.3 V, which should be related with the conversion of SnO to Sn and the formation of Li₂O [1], indicating that tin mainly exists in the form of SnO in TE-230. An oxidation wave centered at 0.5 V can be seen in all the CVs of above three composites, which is associated with the dealloying process of Sn with Li [22]. For TE-450 reduced for 30 and 60 min,
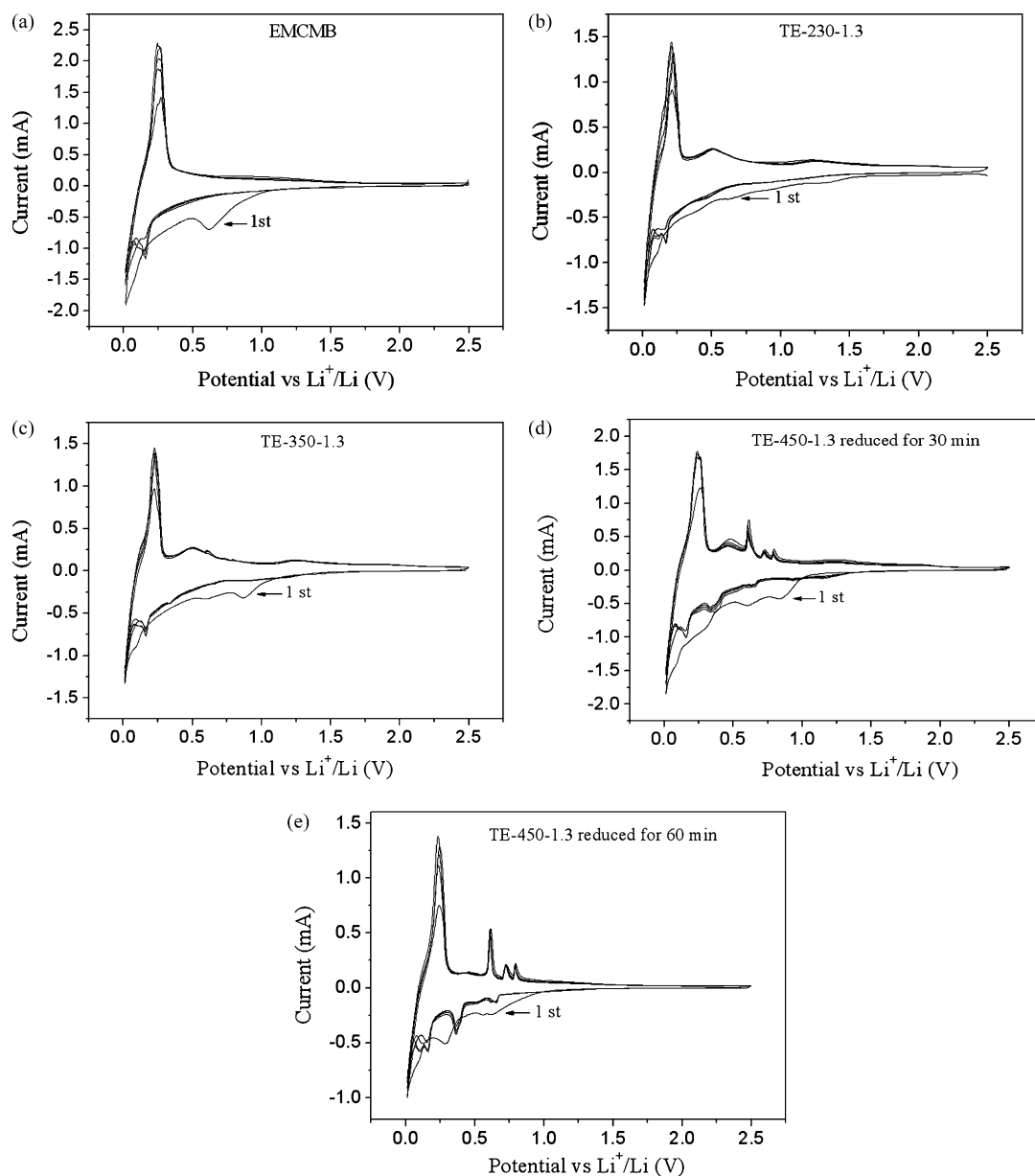
Fig. 3. Cyclic voltammograms of (a) EMCMB, (b) TE-230-1.3, (c) TE-350-1.3 and (d, e) TE-450-1.3 reduced for 30 and 60 min at a scanning rate of 0.1 mV s^{-1}, respectively.

three pairs of other reduction/oxidation peaks are observed, at about 0.36/0.62, 0.52/0.72 and 0.65/0.80 V, respectively. Similar voltammetric features have been observed by Guo et al. in the CV of MWNT-Sn electrode [23]. They believe that these peaks originate from the phase transition of Li$_x$Sn$_y$. The CVs of all samples indicate that both EMCMB and tin are electrochemically active versus lithium, so the capacity of these composite electrodes should be higher than that of common graphite electrode, which was verified by the following galvanostatical tests.

Cycle performances of TE-230 with different loading amount of tin oxides are illustrated in Fig. 4. It can be seen that, at the current density of 0.2 mA cm^{-2}, TE-230-0.5, TE-230-1.3 and TE-230-2.9 exhibit the first reversible capacities of 372, 401, 516 mAh g^{-1} and the first coulombic efficiency of 68%, 64%, 56%, respectively, i.e., with the increase of loading amount of tin

oxides, the first reversible capacity of the composite increases while their first coulombic efficiency decreases. As discussed before, tin oxides undergo a reduction reaction with lithium to form Li$_2$O and metallic tin during the first insertion step [22,24], which is irreversible in nature and leads to the increase of the first irreversible capacity and the decrease of the first coulombic efficiency of composite. From Fig. 4(a), it is also observed that, TE-230-1.3 exhibits a 94% of the capacity retention over 30 cycles, whereas the TE-230-2.9 only delivers a 56% of the capacity retention over the same cycles. At the high-current density of 0.8 mA cm^{-2}, the similar results are obtained (Fig. 4(b)): TE-230-1.3 electrode has the reversible capacity of about 300 mAh g^{-1} and capacity retention of 84% over 30 cycles. Although the first reversible capacity of TE-230-2.9 (390 mAh g^{-1}) is significantly higher than that of TE-230-1.3,
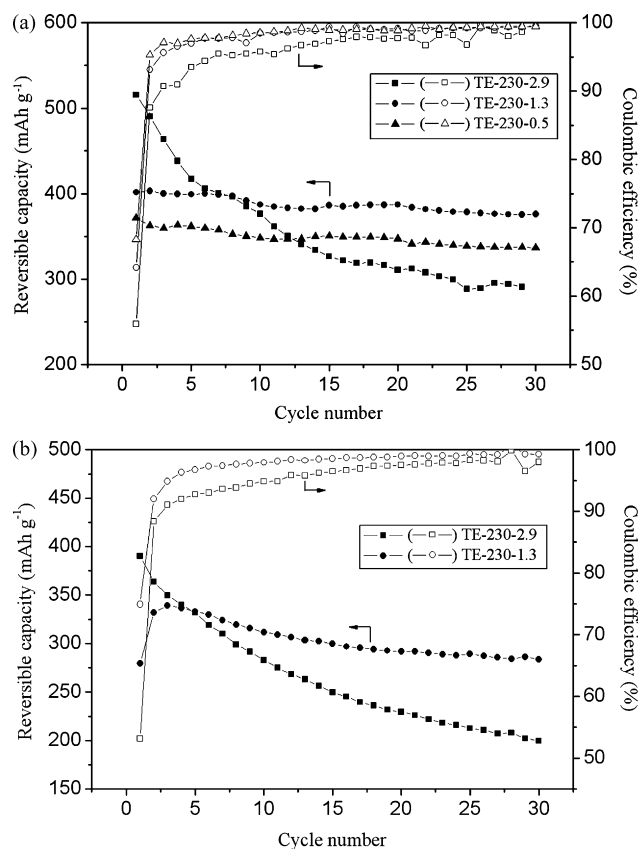
Fig. 4. Cycle performances of TE-230-0.5, TE-230-1.3 and TE-230-2.9 at the current density of (a) 0.2 mA cm^{-2} and (b) 0.8 mA cm^{-2}, respectively.

its capacity retention is only 51%. It should be indicated that, although the density of EMCMB (1.4 g cm^{-3}) is smaller than that of common graphite (2.2 g cm^{-3}), the tin-based EMCMB composites still possess high-volumetric capacities owing to the loading of high-bulk density tin (6.3 g cm^{-3}) or tin oxide. For instance, TE-230-0.5, TE-230-1.3 and TE-230-2.9 show the first reversible volumetric capacities of 557, 642 and 902 mAh cm^{-3}, respectively, which are close to or even higher than that of graphite (626 mAh cm^{-3}) [13]. After 30 cycles, the volumetric capacity of TE-230-1.3 is stable to 601 mAh cm^{-3}, whereas, the volumetric capacity of TE-230-2.9 drastically drops to 509 mAh cm^{-3}, close to that of TE-230-0.5 (505 mAh cm^{-3}).

In order to explore the influence of tin oxides loading on the cycle performance of composites, impedance analysis was carried out on TE-230-0.5, TE-230-1.3 and TE-230-2.9 after 30 cycles. To maintain consistency, all the impedance tests were performed at the open circuit potential of 1.6 V (fully delithiated state). Fig. 5 shows the Nyquist complex plane impedance plots of the composite electrodes. It can be seen that they all comprise two semicircles in high- and medium-frequency ranges and a line inclined at an approximate 45° angle to the real axis in low frequency. According to the previous papers [17,25], the high-frequency semicircle is attributed to SEI film and contact resistance, the semicircle in medium-frequency region is assigned to the charge-transfer impedance on electrode/electrolyte interface, and the inclined line at an approximate 45° angle to the real axis corresponds to the lithium-
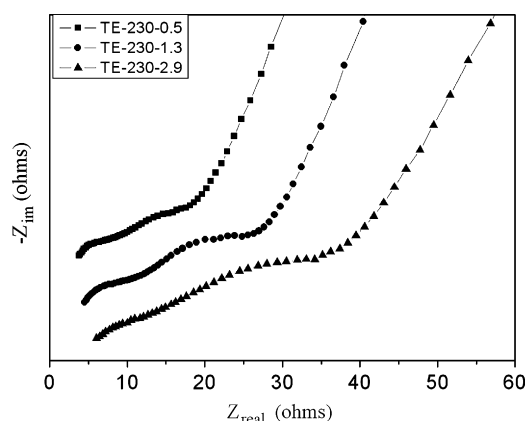

Fig. 5. AC impedance spectra of TE-230-0.5, TE-230-1.3 and TE-230-2.9 electrodes measured at the open potential of 1.6 V after 30 cycles.
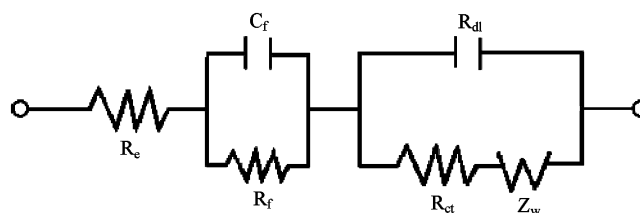

Fig. 6. Randles equivalent circuit for TE-230 electrode/electrolyte interface.

diffusion process within electrode. In our case, the magnitude of both semicircles clearly increases with the increase of tin oxides in composite, indicating the resistance for Li-ion migration through the composite electrode enhances with the increase of tin oxide loading.

These AC impedance spectra for the composite electrodes can be modeled by an equivalent circuit, which is presented in Fig. 6 [17]. R_e is the electrolyte resistance, and C_f and R_f are the capacitance and resistance of the surface film and contact, respectively. C_{dl} and R_{ct} are the double-layer capacitance and charge-transfer resistance, respectively, Z_w is the Warburg impedance related to the diffusion of lithium ions into the bulk of composite electrodes. The exchange current density i_0 can be calculated according to the following equation [17]:

$$i_0 = \frac{RT}{nFR_{ct}} \qquad (2)$$

where R is the gas constant, T the absolute temperature, n the number of transferred electrons and F is the Faraday constant.

The kinetic parameters of the three electrodes are summarized in Table 1. It can be seen that, with the increase of tin oxides in the composites, R_f increases from 3.1 to 6.3 Ω and R_{ct} increases from 2.5 to 7.1 Ω, correspondingly the value of

Table 1
Kinetic parameters of TE-230-0.5, TE-230-1.3 and TE-230-2.9 electrodes at the potential of 1.6 V after 30 cycles

Sample	R_e (Ω)	R_f (Ω)	R_{ct} (Ω)	i_0 (mA cm^{-2})
TE-230-0.5	3.9	3.1	2.5	6.9
TE-230-1.3	4.8	5.1	5.2	3.3
TE-230-2.9	5.7	6.3	7.1	2.4

exchange current density i_0 decreases from 6.9 to 2.4 mA cm^{-2}, suggesting that the SEI film and contact resistance is enhanced and the electrochemical activity of composite electrodes is reduced. This provides the information that the variation of cycle performance of the composites should arise from the resistance change in the composite electrodes. As discussed above, the capacity fading of the composite with higher tin oxides content (TE-230-2.9) is more pronounced than that with lower tin oxides content (TE-230-0.5). The similar phenomenon was also observed by Wang et al. [14] when they investigated the cycle performance of SnO$_2$–graphite composites. They believed that this was most likely due to the easy and increased agglomeration of SnO$_2$ particles in composites with higher tin oxide contents. In our case, the poorer cyclability of TE-230-2.9 should be ascribed to the same reason. The agglomeration of tin oxide particles in TE-230-2.9 must result in the increase of the charge-transfer resistance and the decrease of the electrochemical activity of tin oxides, which is well consistent with the fitting results of the impedance spectra.

The cycle performances of TE-230, TE-350, TE-450 reduced for 30 and 60 min at the current density of 0.2 mA cm^{-2} are also compared, which are shown in Fig. 7. TE-230 and TE-350 display the first reversible capacities of 401 and 419 mAh g^{-1}, respectively, and the former exhibits the most stable cyclability with only 0.2% capacity loss/cycle. In contrast, TE-450 reduced for 30 and 60 min deliver lower reversible capacities and higher capacity loss (0.7% and 0.6% loss/cycle, respectively). The above results indicate the cyclability of these composites decreases with the enhancing of reduction temperature. The reason for this should be that, with the increase of reduction temperature from 230 to 450 °C, tin oxides in the cracks between carbon layers are reduced to the metallic tin. Because of the flowability, some tin particles will escape from the carbon layers and aggregate on the surface of EMCMB leading to the formation of large size particles, which was confirmed from the FE-SEM images and XRD analysis. Although EMCMB can provide a facile environment for the dispersion of tin oxide particles between carbon layers, it cannot efficiently obstruct the agglomeration of tin particles on the surface of EMCMB. Therefore, searching for a suitable matrix and maintaining appropriate

metallic Sn particle sizes in the matrix are the key factors for the improvement of cycle properties of Sn-based negative electrodes.

4. Conclusions

EMCMB used as the matrix of tin or tin oxides was successfully prepared from graphitized MCMB by intercalation reaction and expansion treatment. The loading amount of tin or tin oxides in tin-based EMCMB composites could be altered by changing the concentration of SnCl$_2$ solution and the existing state of tin could be controlled by reduction temperature and time. Tin exists in the form of oxidation states (Sn(II) and Sn(IV)) at lower reduction temperature (below 350 °C) and metallic Sn after reduction at higher temperature (above 450 °C), respectively.

The electrochemical tests showed that loading amount of tin or tin oxides and reduction temperature had great influences on the reversible capacity and cycle performance of these composites when using as negative electrode material for lithium-ion batteries. TE-230 with appropriate loading amount of tin oxides not only exhibited the high first reversible gravimetric capacity of 401 mAh g^{-1} and an excellent cyclability with only 0.2% capacity loss/cycle at the low current density, but also showed a stable cycle performance at the higher current density, indicating EMCMB is a suitable matrix for Sn-containing negative electrodes.

References

[1] W. Choi, J.Y. Lee, B.H. Jung, H.S. Lim, J. Power Sources 136 (2004) 154.
[2] J. Read, D. Foster, J. Wolfenstine, W. Behl, J. Power Sources 96 (2001) 277.
[3] T. Moon, C. Kim, S.T. Hwang, B. Park, Electrochem. Solid-State Lett. 9 (2006) A408.
[4] R. Zhang, J.Y. Lee, Z.L. Liu, J. Power Sources 112 (2002) 596.
[5] J.Y. Lee, R. Zhang, Z. Liu, Electrochem. Solid-State Lett. 3 (2000) 167.
[6] Y. Wang, J.Y. Lee, T.C. Deivaraj, J. Electrochem. Soc. 151 (2004) A1804.
[7] G.X. Wang, J. Yao, H.K. Liu, S.X. Dou, J.H. Ahn, Electrochim. Acta 50 (2004) 517.
[8] I. Grigoriants, L. Sominski, H. Li, I. Ifargan, D. Aurbach, A. Gedanken, Chem. Commun. 7 (2005) 921.
[9] J. Fan, T. Wang, C. Yu, B. Tu, Z. Jiang, D. Zhao, Adv. Mater. 16 (2004) 1432.
[10] I. Grigoriants, A. Soffer, G. Salitra, D. Aurbach, J. Power Sources 146 (2005) 185.
[11] T. Morishita, T. Hirabayashi, T. Okuni, N. Ota, M. Inagaki, J. Power Sources 160 (2006) 638.
[12] A. Ulus, Y. Rosenberg, L. Burstein, E. Peled, J. Electrochem. Soc. 149 (2002) A635.
[13] B. Veeraraghavan, A. Durairajan, B. Haran, B. Popov, R. Guidotti, J. Electrochem. Soc. 149 (2002) A675.
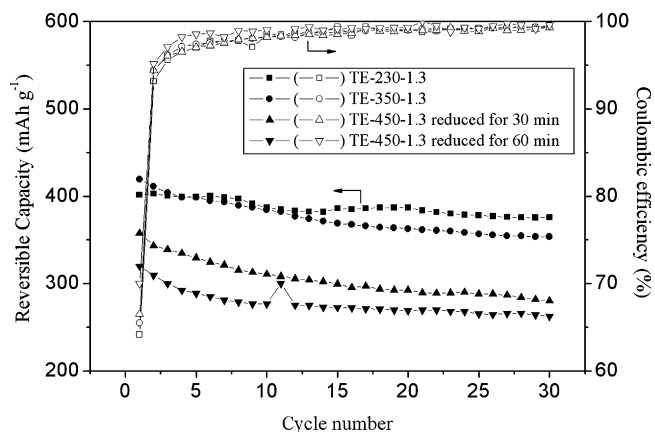[14] Y. Wang, J.Y. Lee, B.H. Chen, J. Electrochem. Soc. 151 (2004) A563.

Fig. 7. Cycle performances of TE-230-1.3, TE-350-1.3 and TE-450-1.3 reduced for 30 and 60 min at the current density of 0.2 mA cm^{-2}.

[15] A. Sivashanmugam, T.P. Kumar, N.G. Renganathan, S. Gopukumar, M. Wohlfahrt-Mehrens, J. Grarche, J. Power Sources 144 (2005) 197.

[16] S. Zhang, P. Shi, Electrochim. Acta 49 (2004) 1475.

[17] S. Yang, H. Song, X. Chen, Electrochem. Commun. 8 (2006) 137.

[18] S. Yang, H. Song, X. Chen, Carbon 44 (2006) 730.

[19] M.S. Moreno, G. Punte, G. Rigotti, R.C. Mercader, A.D. Weisz, M.A. Blesa, Solid State Ionics 144 (2001) 81.

[20] Y.N. Nuli, S.L. Zhao, Q.Z. Qin, J. Power Sources 114 (2003) 113.

[21] J. Yao, G.X. Wang, J.H. Ahn, H.K. Liu, S.X. Dou, J. Power Sources 114 (2003) 292.

[22] N. Li, C.R. Martin, J. Electrochem. Soc. 148 (2001) A164.

[23] Z.P. Guo, Z.W. Zhao, H.K. Liu, S.X. Dou, Carbon 43 (2005) 1392.

[24] I.A. Countney, J.R. Dahn, J. Electrochem. Soc. 144 (1997) 2045.

[25] S. Yang, H. Song, X. Chen, A.V. Okotrub, L.G. Bulusheva, Electrochim. Acta 52 (2007) 5286.